A cell-centered Arbitrary Lagrangian Eulerian method for two-dimensional multimaterial problems

Application to Inertial Confinement Fusion modeling in the direct drive context

Pierre-Henri Maire, maire@celia.u-bordeaux1.fr

UMR CELIA, CNRS, University Bordeaux 1, CEA,

351, cours de la Libération, 33405 Talence, France

Collaborations: Rémi Abgrall, Jérôme Breil, Stéphane Galera, Boniface NKonga

Outline

- Introduction and motivations
- Lagrangian phase
- Numerical results
- Rezoning phase
  - interior nodes
  - boundary and interfaces nodes
- Remapping phase
- Numerical results
- Conclusions and perspectives

Introduction and motivations

- ICF plasma is created by laser interaction with target
- ICF target is the assembly of multimaterial layers with high aspect ratios
- Multimaterial flows with large displacements, strong shocks and rarefaction waves
- Simulations with large changes of computational domain volume and shape (animation)
- Lagrangian formulation is well adapted to ICF flows

  Mesh moves with the fluid
  Shock resolution is increased
  No mass flux between cell
  Free surfaces are naturaly treated
  Interfaces are sharply resolved

- However for too large deformations (shear and vorticity) it appears a lack of robustness (mesh tangling)
- It can be treated by using an Arbitrary Lagrangian Eulerian (ALE) strategy

ALE strategy

- Lagrangian phase
  - New second order cell-centered Lagrangian scheme*
  - Conservative and entropy consistent
  - Cell-centered momentum easier to handle in view of ALE
- Rezoning phase
  - Improvement of geometric quality of the grid
  - Quasi Lagrangian interface tracking using Bezier curves
- Remapping phase
  - Conservative transfer from the Lagrangian mesh to the rezoned
  - Swept displacement face flux computation
  - Second order accuracy

*Ref: P.-H. Maire, R. Abgrall, J. Breil, J. Ovadia. *A cell-centered Lagrangian scheme for two-dimensional compressible flow problems*, to appear in SIAM Journal of Scientific Computing (2007); https://hal.inria.fr/inria-00113542.

Governing equations

- ALE form of the compressible Euler equations

For a moving control volume $\Omega(t)$ whose boundary's velocity is $\dot{\boldsymbol{X}}$

$$\frac{d}{dt}\int_{\Omega(t)} \mathrm{d}\Omega - \int_{\partial\Omega(t)} \dot{\boldsymbol{X}}\cdot\boldsymbol{N}\,\mathrm{d}l = 0, \qquad \text{geometric conservation law}$$

$$\frac{d}{dt}\int_{\Omega(t)} \rho\,\mathrm{d}\Omega + \int_{\partial\Omega(t)} \rho\left(\boldsymbol{V}-\dot{\boldsymbol{X}}\right)\cdot\boldsymbol{N}\rho\,\mathrm{d}l = 0,$$

$$\frac{d}{dt}\int_{\Omega(t)} \rho\boldsymbol{V}\,\mathrm{d}\Omega + \int_{\partial\Omega(t)} \left[\left(\boldsymbol{V}-\dot{\boldsymbol{X}}\right)\cdot\boldsymbol{N}\rho\boldsymbol{V}+P\boldsymbol{N}\right]\,\mathrm{d}l = \boldsymbol{0},$$

$$\frac{d}{dt}\int_{\Omega(t)} \rho E\,\mathrm{d}\Omega + \int_{\partial\Omega(t)} \left[\left(\boldsymbol{V}-\dot{\boldsymbol{X}}\right)\cdot\boldsymbol{N}\rho E+P\boldsymbol{V}\cdot\boldsymbol{N}\right]\,\mathrm{d}l = 0.$$

Equation of state: $P \equiv P(\rho,\varepsilon)$ where $\varepsilon = E - \frac{1}{2}\mid \boldsymbol{V}\mid^2$.

For $\dot{\boldsymbol{X}} = \boldsymbol{V}$ (resp. $\dot{\boldsymbol{X}} = \boldsymbol{0}$) we recover the Lagrangian (resp. Eulerian) formulation.

Lagrangian phase

- Evolution equations for the discrete unknowns $(\tau_c = \frac{1}{\rho_c}, \boldsymbol{V_c}, E_c)$

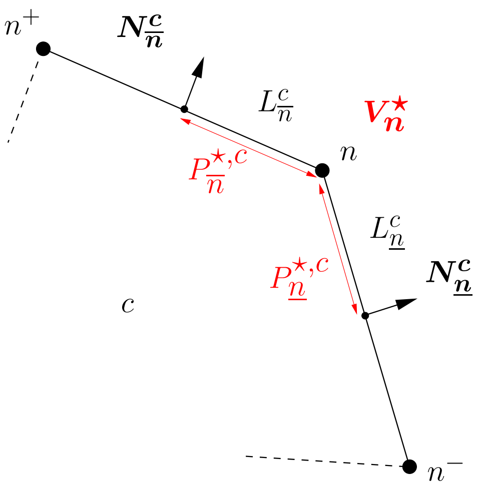

$$m_c \frac{d}{dt}\tau_c - \sum_{n\in\mathcal{N}(c)} \left(L^c_{\underline{n}} \boldsymbol{N}^{\boldsymbol{c}}_{\underline{\boldsymbol{n}}} + L^c_{\overline{n}} \boldsymbol{N}^{\boldsymbol{c}}_{\overline{\boldsymbol{n}}} \right) \cdot \boldsymbol{V}^\star_{\boldsymbol{n}} = 0,$$

$$m_c \frac{d}{dt}\boldsymbol{V_c} + \sum_{n\in\mathcal{N}(c)} \left(L^c_{\underline{n}} P^{\star,c}_{\underline{n}} \boldsymbol{N}^{\boldsymbol{c}}_{\underline{\boldsymbol{n}}} + L^c_{\overline{n}} P^{\star,c}_{\overline{n}} \boldsymbol{N}^{\boldsymbol{c}}_{\overline{\boldsymbol{n}}} \right) = \boldsymbol{0},$$

$$m_c \frac{d}{dt}E_c + \sum_{n\in\mathcal{N}(c)} \left(L^c_{\underline{n}} P^{\star,c}_{\underline{n}} \boldsymbol{N}^{\boldsymbol{c}}_{\underline{\boldsymbol{n}}} + L^c_{\overline{n}} P^{\star,c}_{\overline{n}} \boldsymbol{N}^{\boldsymbol{c}}_{\overline{\boldsymbol{n}}} \right) \cdot \boldsymbol{V}^\star_{\boldsymbol{n}} = 0,$$

where $\mathcal{N}(c)$ is the set of vertices of cell c.

- Node motion

$$\frac{d}{dt}\boldsymbol{X_n} = \boldsymbol{V}^\star_{\boldsymbol{n}}, \quad \boldsymbol{X_n}(0) = \boldsymbol{x_n}.$$

Construction of a nodal solver to evaluate the nodal fluxes $\boldsymbol{V}^\star_{\boldsymbol{n}}$, $P^{\star,c}_{\underline{n}}$ and $P^{\star,c}_{\overline{n}}$.

Lagrangian phase

- Computation of the nodal fluxes $\boldsymbol{V}^{\star}_{\boldsymbol{n}}$, $P^{\star,c}_{\underline{n}}$ and $P^{\star,c}_{\overline{n}}$

Let $\mathsf{M}^c_n = Z_c \left(L^c_{\underline{n}} \boldsymbol{N}^{\boldsymbol{c}}_{\underline{\boldsymbol{n}}} \otimes \boldsymbol{N}^{\boldsymbol{c}}_{\underline{\boldsymbol{n}}} + L^c_{\overline{n}} \boldsymbol{N}^{\boldsymbol{c}}_{\overline{\boldsymbol{n}}} \otimes \boldsymbol{N}^{\boldsymbol{c}}_{\overline{\boldsymbol{n}}} \right)$

$$\boldsymbol{V}^{\star}_{\boldsymbol{n}} = \left(\sum_{c \in \mathcal{C}(n)} \mathsf{M}^c_n \right)^{-1} \sum_{c \in \mathcal{C}(n)} \left[\left(L^c_{\underline{n}} \boldsymbol{N}^{\boldsymbol{c}}_{\underline{\boldsymbol{n}}} + L^c_{\overline{n}} \boldsymbol{N}^{\boldsymbol{c}}_{\overline{\boldsymbol{n}}} \right) P_c + \mathsf{M}^c_n \boldsymbol{V}_{\boldsymbol{c}} \right],$$

where $\mathcal{C}(n)$ is the set of the cells sharing node n.

$$P_c - P^{\star,c}_{\underline{n}} = Z_c \left(\boldsymbol{V}^{\star}_{\boldsymbol{n}} - \boldsymbol{V}_{\boldsymbol{c}} \right) \cdot \boldsymbol{N}^{\boldsymbol{c}}_{\underline{\boldsymbol{n}}},$$
$$P_c - P^{\star,c}_{\overline{n}} = Z_c \left(\boldsymbol{V}^{\star}_{\boldsymbol{n}} - \boldsymbol{V}_{\boldsymbol{c}} \right) \cdot \boldsymbol{N}^{\boldsymbol{c}}_{\overline{\boldsymbol{n}}},$$

Riemann invariants

We can check that these fluxes lead to a conservative and entropy consistent scheme. For 1D flows, we recover exactly the Godunov acoustic fluxes.

Lagrangian phase

- Second order extension
  - Piecewise linear reconstruction $\phi_c(\boldsymbol{X}) = \phi_c + \boldsymbol{\nabla}\phi_c \cdot (\boldsymbol{X} - \boldsymbol{X_c})$
  - Computation of $\boldsymbol{\nabla}\phi_c$ by a least squares procedure
  - Reconstruction exact for linear fields
  - Monotony ensured by slope limiters so that

$$\min_{k \in \mathcal{C}(c)} \phi_k \leq \phi_c(\boldsymbol{X_n}) \leq \max_{k \in \mathcal{C}(c)} \phi_k,$$

    where $\mathcal{C}(c)$ is the set of the nearest neighbors of cell c.
  - Extrapolated values of P and $\boldsymbol{V}$ at the nodes for the nodal solver
  - Explicit time discretization by a 2 steps Runge-Kutta procedure

Numerical results

- Sedov test case on a 50×50 Cartesian grid

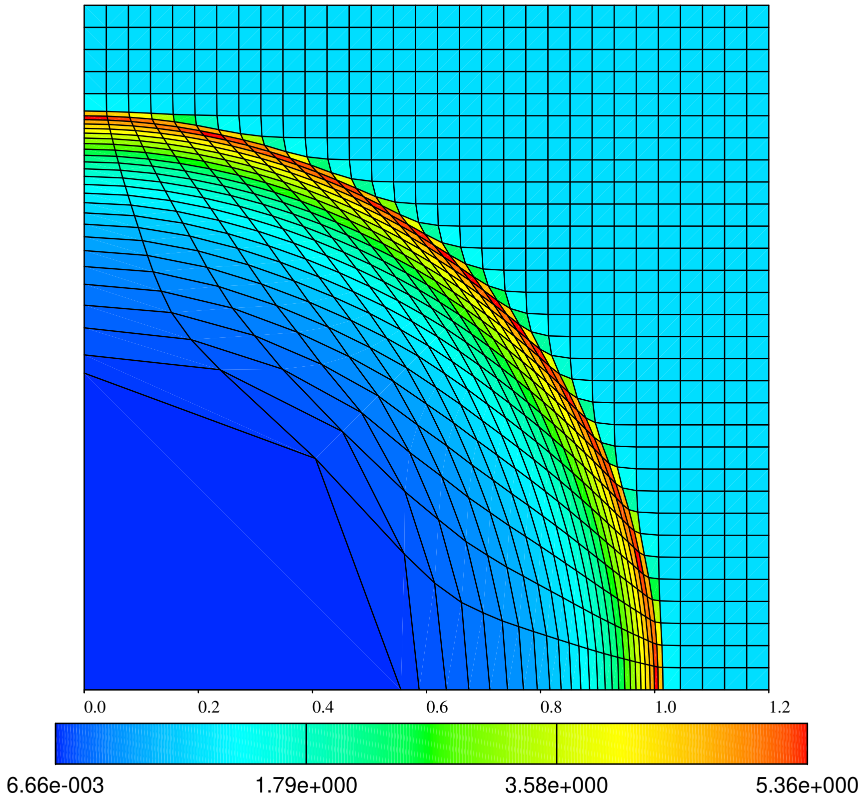

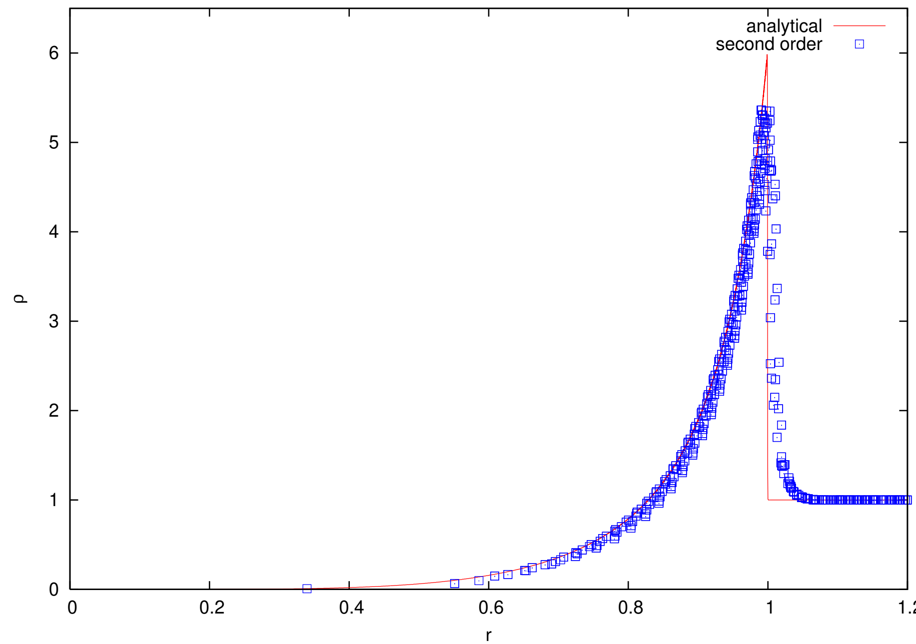

Density map (left) and density in all the cells (right) at $t = 1$.

Ref : R. LOUBÈRE, M.J. SHASHKOV, *A subcell remapping method on staggered polygonal grids for ALE methods*, JCP **209** (2005) 105-138.

Numerical results

- Sedov test case on a polygonal grid

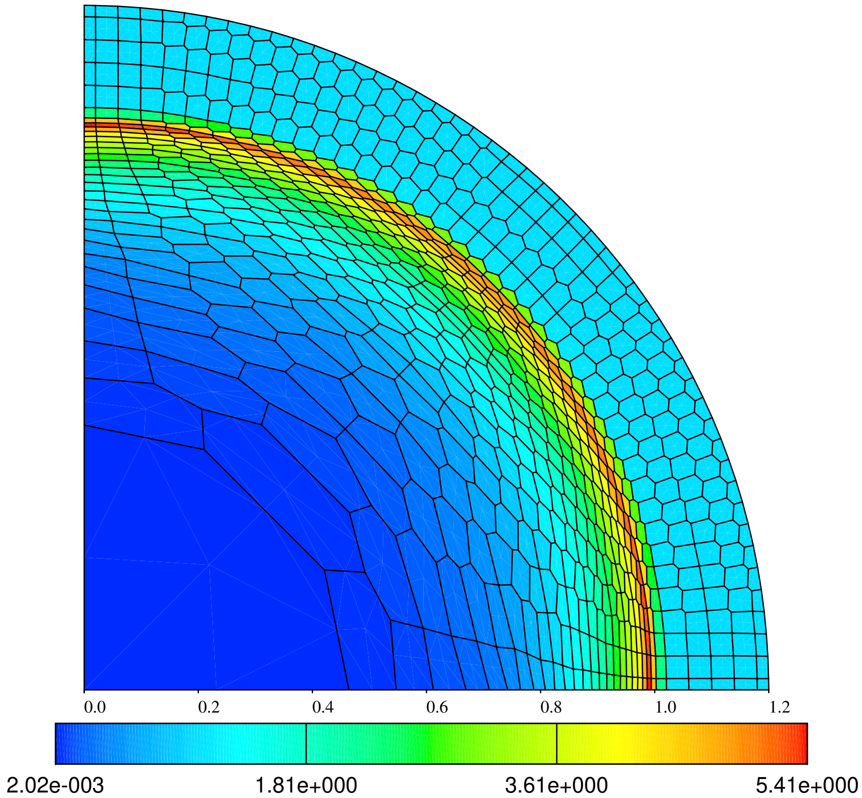

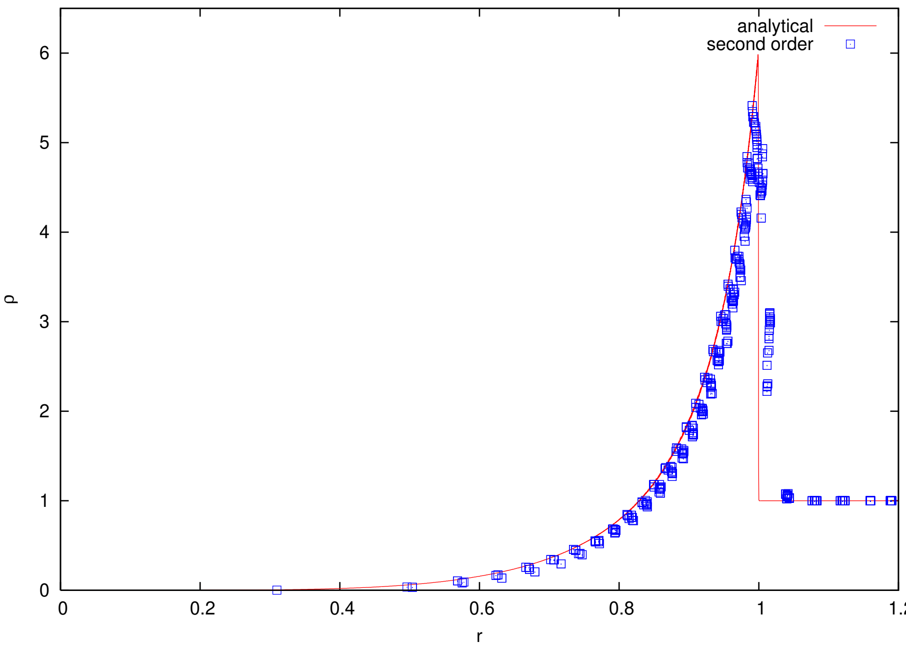

Density map (left) and density in all the cells (right) at $t = 1$.

Numerical results

- Cylindrical Noh test case on a non-conformal grid

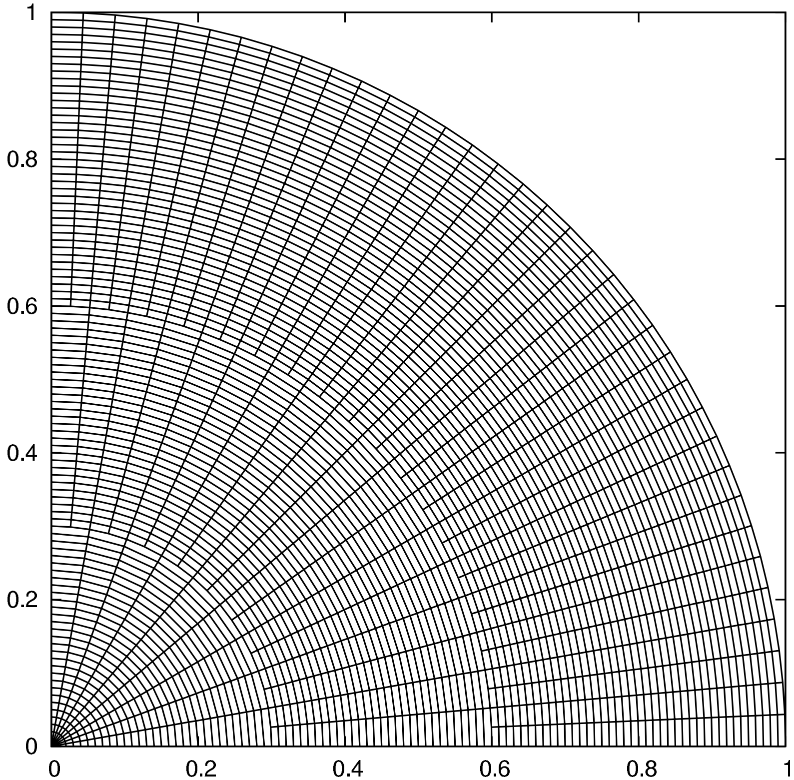

Initial mesh

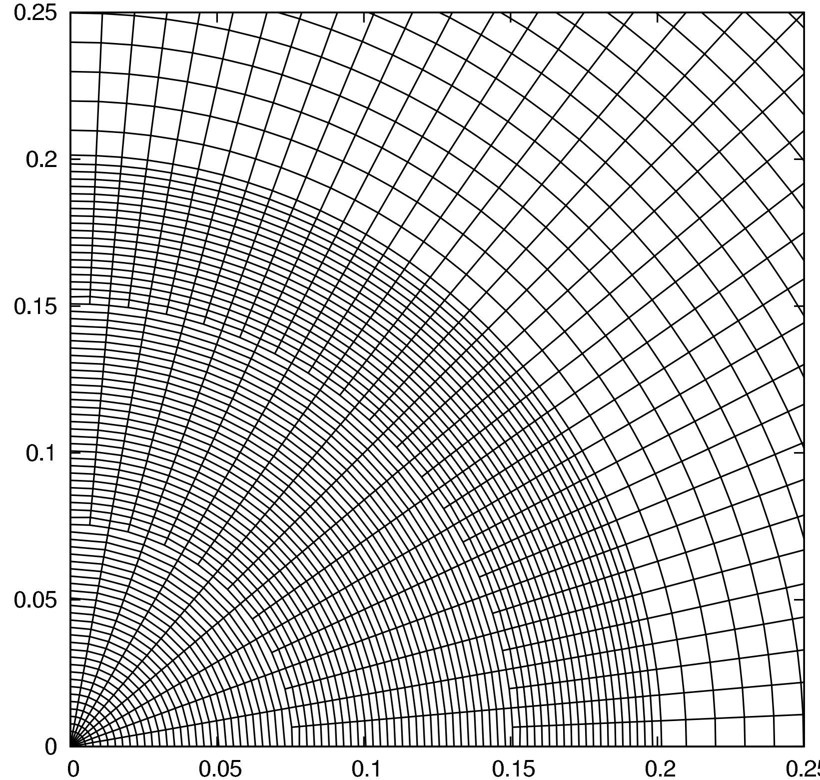

Zoom on the final mesh

Non-conformal mesh with 2 levels of refinement, 2250 cells mix of triangles, quadrangles and pentagons.

Numerical results

- Cylindrical Noh test case on a non-conformal grid

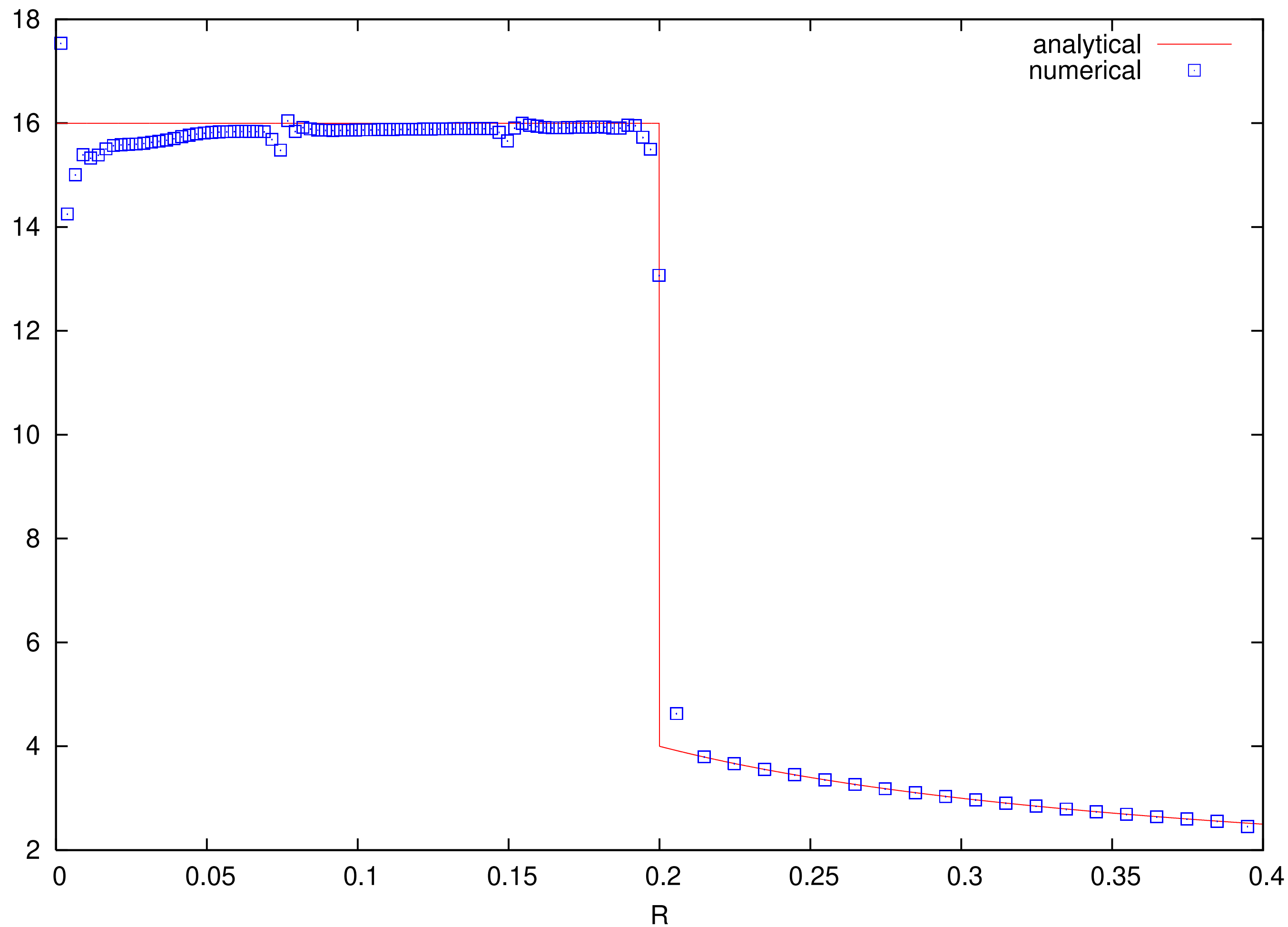

Density in all the cells at $t = 0.6$

Rezoning phase

- Unstructured mesh quality optimization
  - ◇ Construct local nodally based objective functions [Knupp (IJNME, 2000)]
  - ◇ Minimize separately each of the local objective function
  - ◇ Iterate over all the nodes of the mesh
- Treatment of boundary and interface nodes
  - ◇ Free boundaries and interfaces are fitted with Bezier curves
  - ◇ Nodes are assigned to move on these Bezier curves
  - ◇ It leads to constrained minimization problems
- Mesh untangling by combination of feasible set method and numerical optimization [Vachal, Garimella, Shashkov (JCP, 2004)].
- Main issue: keep the rezoned mesh as close to Lagrangian as possible by using relaxation criteria related to mesh quality measurements [Ph. Hoch (2007)]

Mesh optimization

- Nodal objective function

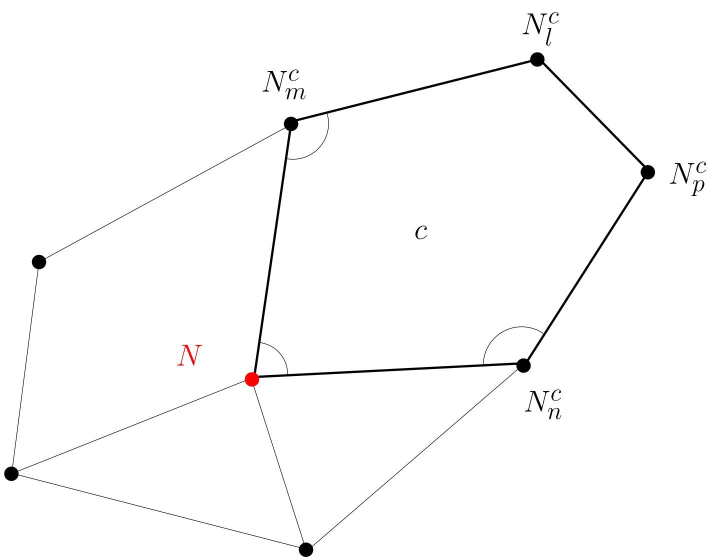

Jacobian matrices related to c and $N(x, y)$

$$\mathsf{J}^{\mathsf{c}} = (\boldsymbol{N}\boldsymbol{N}_{\boldsymbol{n}}^{\boldsymbol{c}}, \boldsymbol{N}\boldsymbol{N}_{\boldsymbol{m}}^{\boldsymbol{c}})$$

$$\mathsf{J}_{\mathsf{n}}^{\mathsf{c}} = \left(\boldsymbol{N}_{\boldsymbol{n}}^{\boldsymbol{c}}\boldsymbol{N}_{\boldsymbol{p}}^{\boldsymbol{c}}, \boldsymbol{N}_{\boldsymbol{n}}^{\boldsymbol{c}}\boldsymbol{N}\right)$$

$$\mathsf{J}_{\mathsf{m}}^{\mathsf{c}} = (\boldsymbol{N}_{\boldsymbol{m}}^{\boldsymbol{c}}\boldsymbol{N}, \boldsymbol{N}_{\boldsymbol{m}}^{\boldsymbol{c}}\boldsymbol{N}_{\boldsymbol{l}}^{\boldsymbol{c}})$$

The displacement of $N(x, y)$ is computed by minimizing

$$F(x, y) = \sum_{c \in \mathcal{C}(N)} \frac{\| \mathsf{J}^{\mathsf{c}} \|^2}{| \det \mathsf{J}^{\mathsf{c}} |} + \frac{\| \mathsf{J}_{\mathsf{n}}^{\mathsf{c}} \|^2}{| \det \mathsf{J}_{\mathsf{n}}^{\mathsf{c}} |} + \frac{\| \mathsf{J}_{\mathsf{m}}^{\mathsf{c}} \|^2}{| \det \mathsf{J}_{\mathsf{m}}^{\mathsf{c}} |}$$

with a Newton procedure (single step towards the minimum).
This objective function is closely related to the Winslow smoother.

Mesh optimization

- Treatment of interface nodes

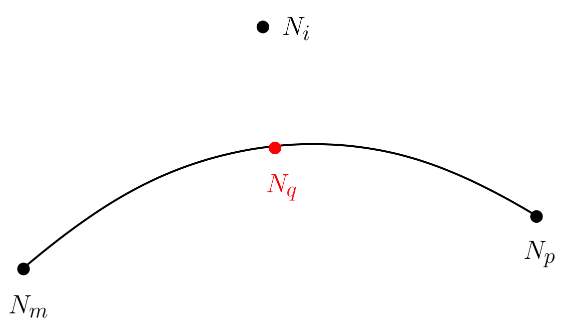

Interpolated Bezier curve for $t \in [0,1]$

$$x(t) = (1-t)^2 x_m + 2(1-t)t x_i + t^2 x_p$$
$$y(t) = (1-t)^2 y_m + 2(1-t)t y_i + t^2 y_p$$

Control point N_i is computed such that N_q is on the curve with parameter $t_q = 0.5$.

The displacement of N_q is computed by minimizing the objective function

$$\Phi(t) = F[x(t), y(t)], \text{ with } t \in]0,1[$$

- Treatment of symmetry axis nodes

Symmetry axis is the straight line $ax + by + c = 0$, then the displacement of N_q is computed by minimizing the objective function $F(x,y) + \Lambda(ax + by + c)$ where Λ is a Lagrange multiplier.

Relaxation criterion

- Nodal quality (cf. Ph. Hoch talk)

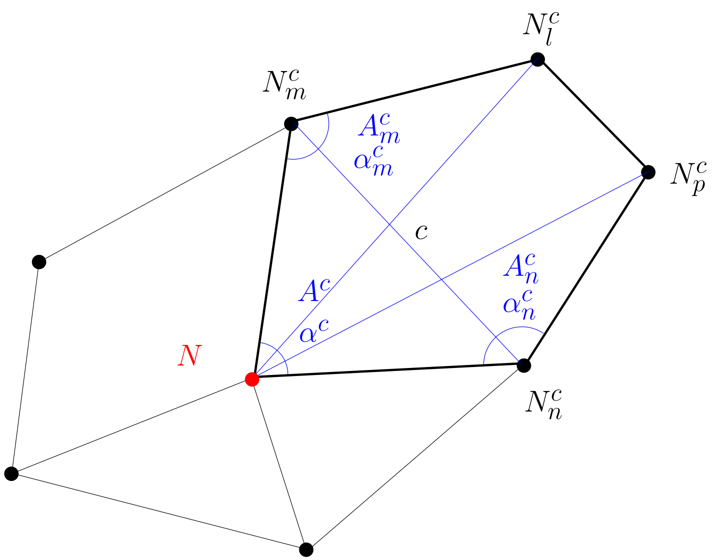

Quality based on angle or area

$$Q_N^{\sin} = \frac{\min_{c \in \mathcal{C}(N)} \left[\sin \alpha_m^c, \sin \alpha^c, \sin \alpha_n^c\right]}{\max_{c \in \mathcal{C}(N)} \left[\sin \alpha_m^c, \sin \alpha^c, \sin \alpha_n^c\right]}$$

$$Q_N^{\text{area}} = \frac{\min_{c \in \mathcal{C}(N)} \left[A_m^c, A^c, A_n^c\right]}{\max_{c \in \mathcal{C}(N)} \left[A_m^c, A^c, A_n^c\right]}$$

For quadrangular grids with high aspect ratios we use $Q_N^{\sin}$ quality. The relaxed mesh is defined by

$$\boldsymbol{X}_N^{\text{rel}} = \omega_N \boldsymbol{X}_N^{\text{rez}} + (1 - \omega_N) \boldsymbol{X}_N^{\text{Lag}}, \text{ with } \omega_N = \min\left[1, \max\left(0, \frac{Q_{\max} - Q_N^{\sin}}{Q_{\max} - Q_{\min}}\right)\right]$$

where $Q_{\max} = \sin \theta_{\max}$, $Q_{\min} = \sin \theta_{\min}$ with $\theta_{\min} = 0$ and $\theta_{\max} = \pi/2$.

Remapping phase

- Conservative interpolation of $(\rho, \rho\boldsymbol{V}, \rho E)$ from the Lagrangian mesh to the new relaxed mesh
- Piecewise monotonic linear reconstruction over the Lagrangian mesh
- Remapping expressed in terms of fluxes across cell faces
- Approximate quadrature over regions swept by edges moving from Lagrangian position to the relaxed position
- Integral over new cells=sum of integrals over swept regions
- Cheaper than exact integration for wich intersections is needed

Numerical results

- Three materials instability

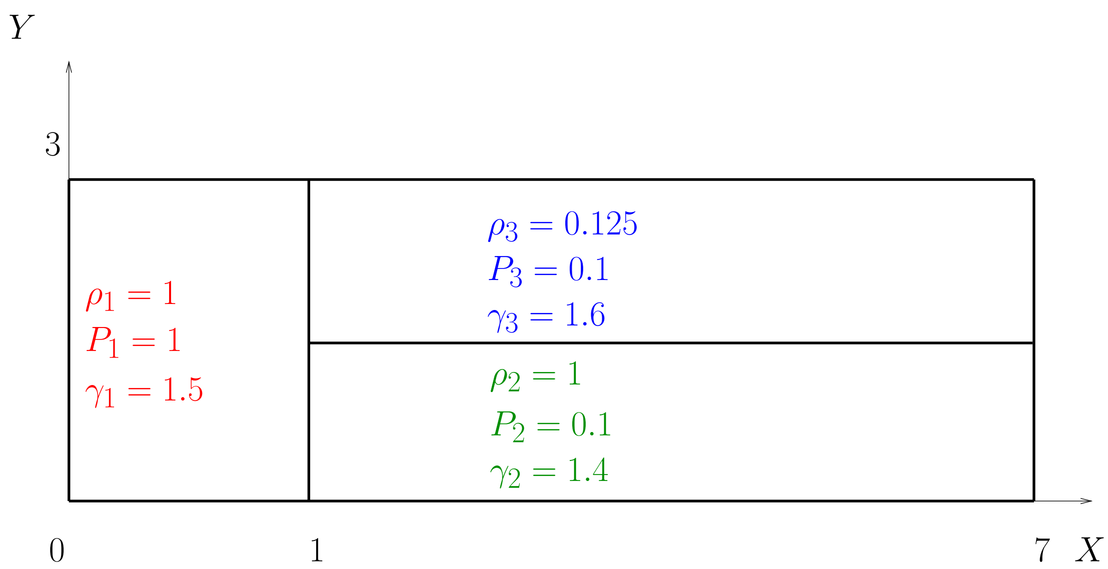

Shock wave interacting with a triple point

- ◇ Cartesian mesh 70×30 cells, $t_{\text{end}} = 5$
- ◇ Lagrange, ALE and Euler second order computations
- ◇ Concentration equations for ALE and Euler
- ◇ Mixture assumption isoP, isoT

Numerical results

- Three materials instability: Lagrangian computation

C_2 map at $t = 2.5$

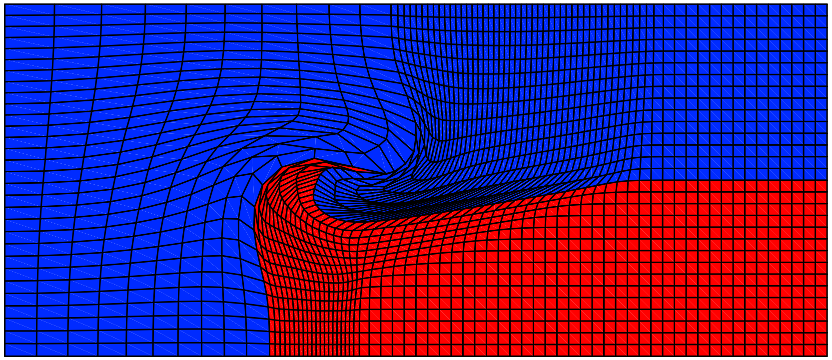

Zoom on the vortex

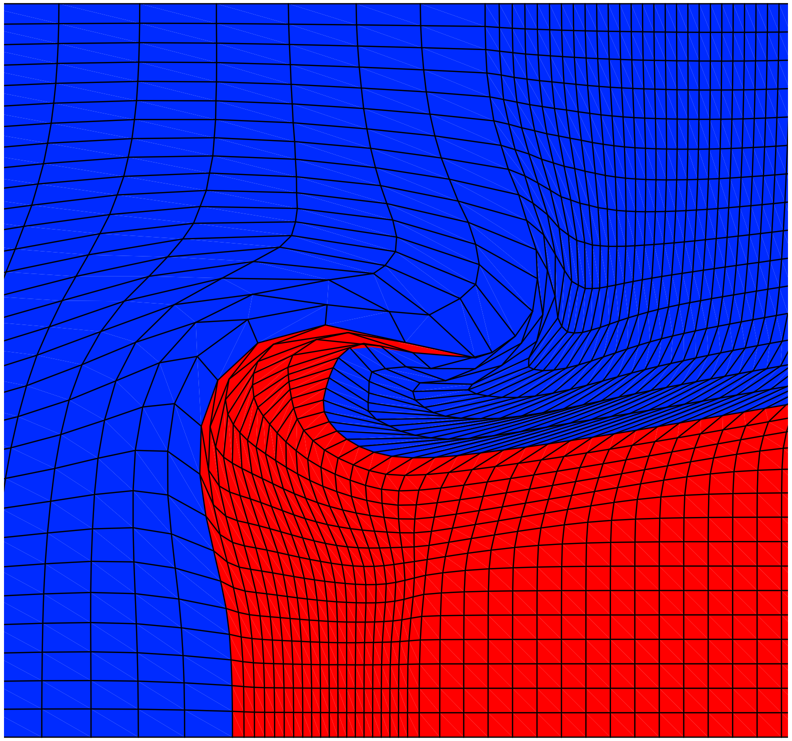

Lagrangian computation fails due to the tangled mesh

Numerical results

- Three materials instability: Lagrange and ALE at $t = 2.5$

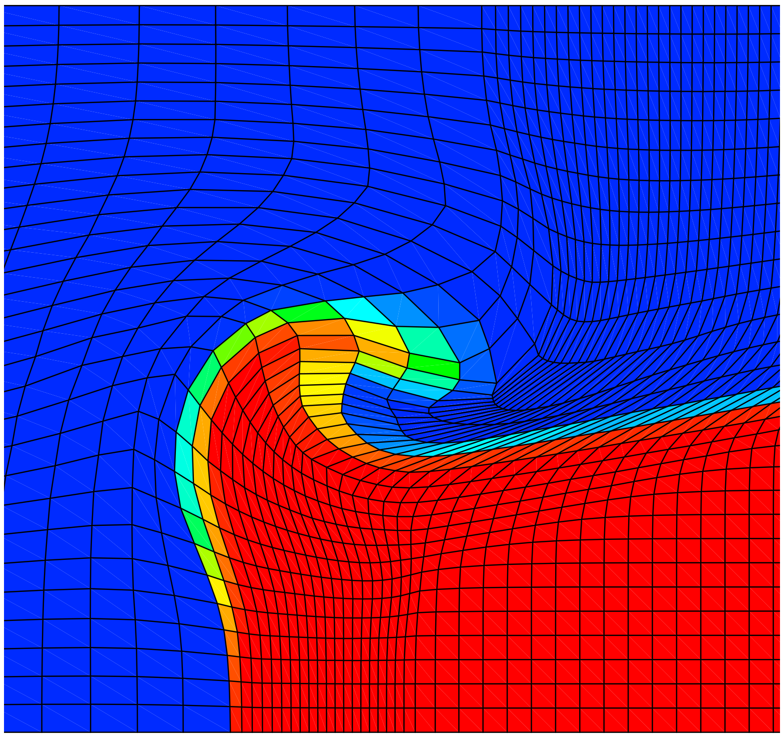

ALE computation

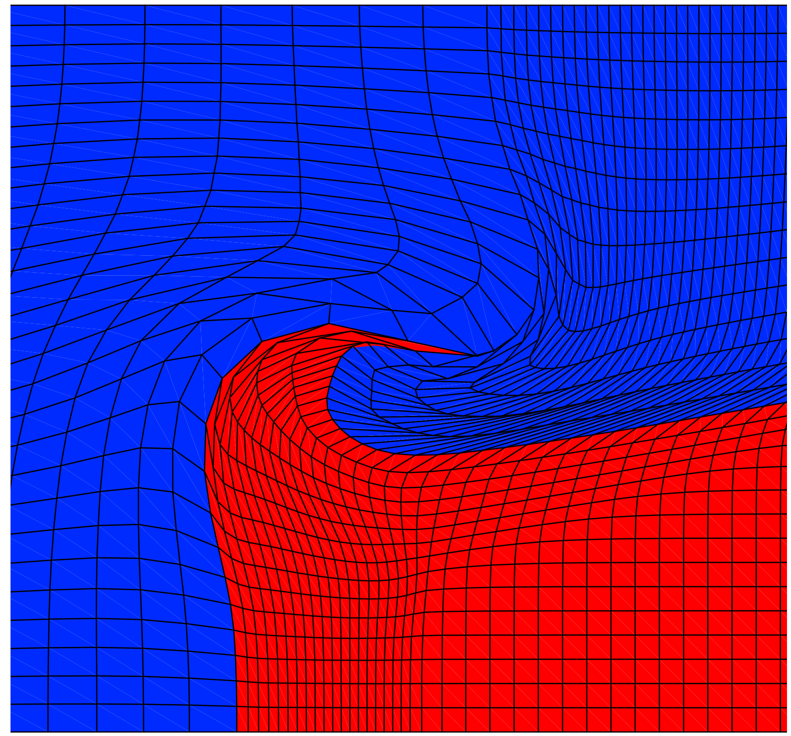

Lagrangian computation

We note the efficiency of the mesh relaxation based on angle criterion

Numerical results

- Three materials instability: ALE and EULER at $t = 2.5$

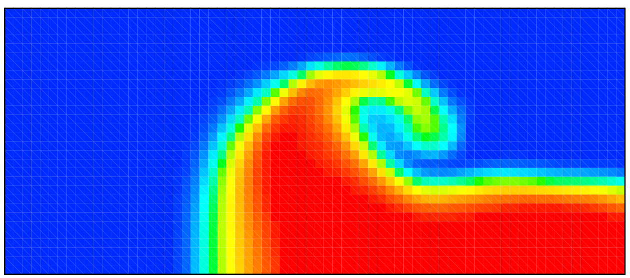

Eulerian computation

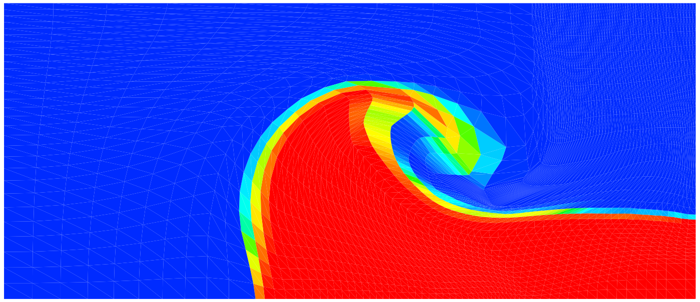

ALE computation

We note the diffusion of the interface in the Eulerian case

Numerical results

- Non-linear phase of Richtmyer-Meshkov instability

Ref : C. MÜGLER, L. HALLO ET AL., *Validation of an ALE Godunov Algorithm for Solutions of the Two-Species Navier-Stokes Equations*, AIAA 96-2068, June 1996.

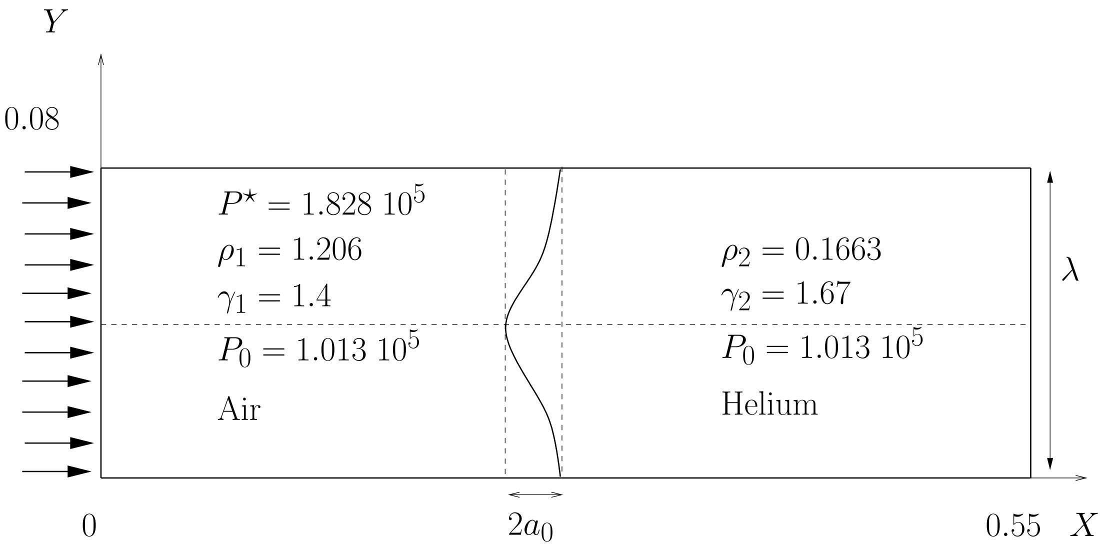

Transmitted shock
Reflected rarefaction wave
$a_0 = 0.32\ 10^{-2}$

- ◇ Initial perturbation $X_{\text{inter}} = 0.4 + a_0 \cos(\frac{2\pi}{\lambda} Y)$
- ◇ ALE second order calculation
- ◇ Mixture assumption isoP, isoT
- ◇ 3 Meshes, cell sizes: $2 \times 2\ mm^2$, $1 \times 1\ mm^2$ and $0.5 \times 0.5\ mm^2$

ALE results

- X-t diagram of the flow

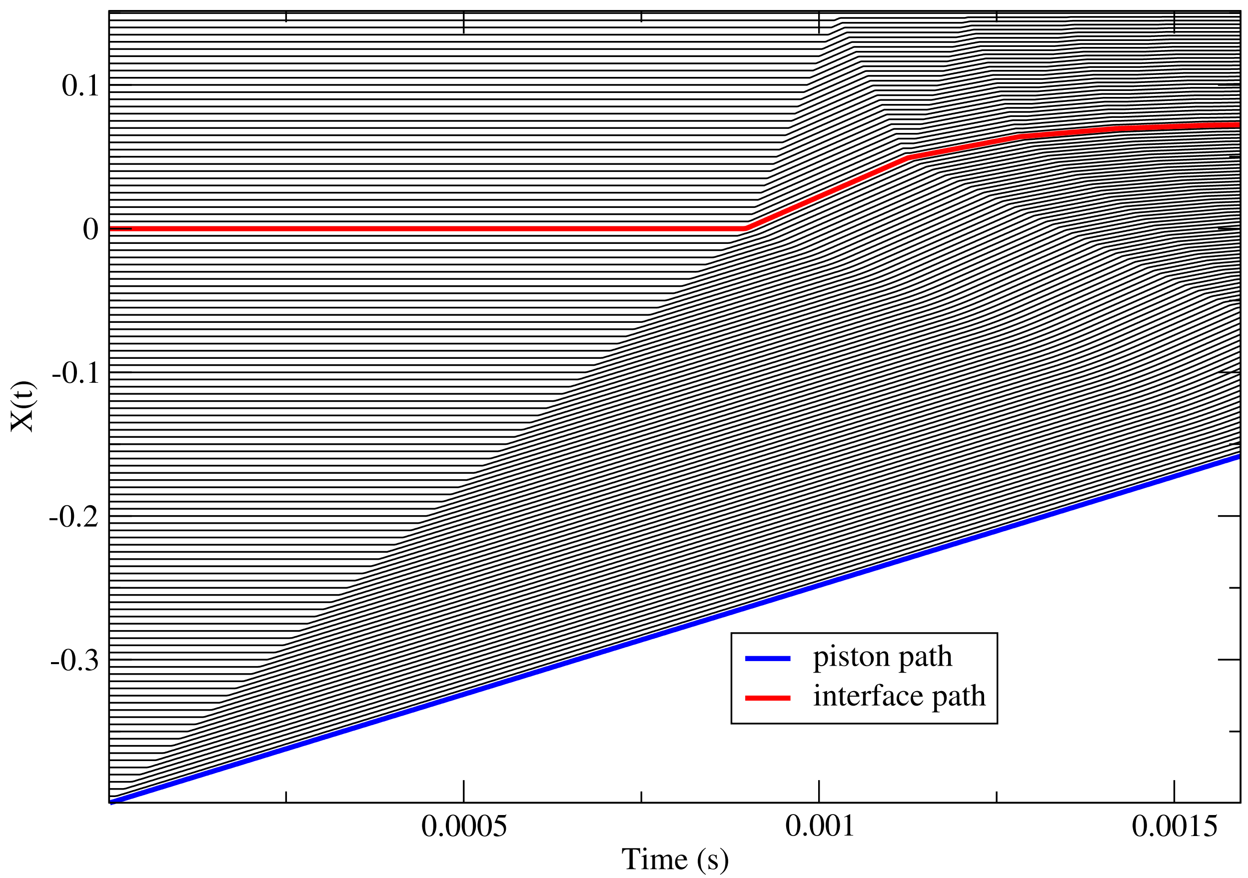

ALE results

- Non-linear phase of Richtmyer-Meshkov instability

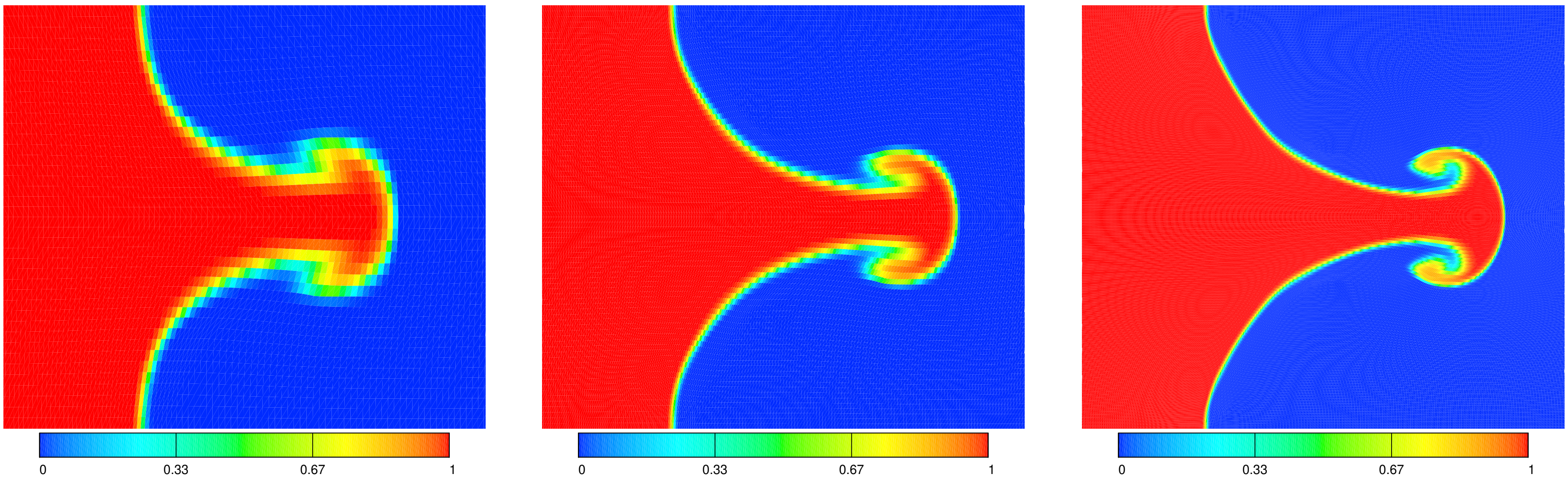

Cell size $2 \times 2\ mm^2$ Cell size $1 \times 1\ mm^2$ Cell size $0.5 \times 0.5\ mm^2$

Concentration maps at $t = 15.973\ 10^{-4}$ s

Experiment restitution

- Characterization of non local heat transport

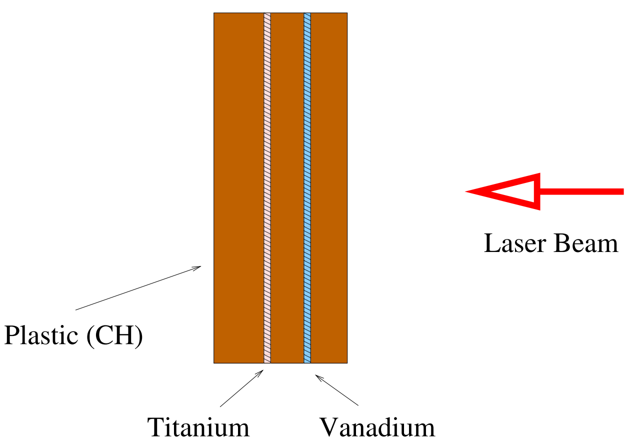

- ◇ Plastic target with Vanadium and Titanium markers of $200\ \mu\mathrm{m}$ thickness
- ◇ Vanadium marker of $0.1\ \mu\mathrm{m}$ thickness at $5\ \mu\mathrm{m}$
- ◇ Titanium marker of $0.1\ \mu\mathrm{m}$ thickness at $15\ \mu\mathrm{m}$
- ◇ Include steady state radiative physics and transverse MHD
- ◇ LIL laser beam : $\lambda = 0.35\ \mu\mathrm{m}$, maximal intensity $1.\ 10^{15}\mathrm{W\ cm}^{-2}$
- ◇ ALE computation with Bezier curves for interface and free boundary tracking

Ref : G. Schurtz et al., *Revisiting nonlocal electron-energy transport in Inertial Fusion conditions*, PRL **98**, 2007.

Experiment restitution

- Map of ionization level and electron temperature

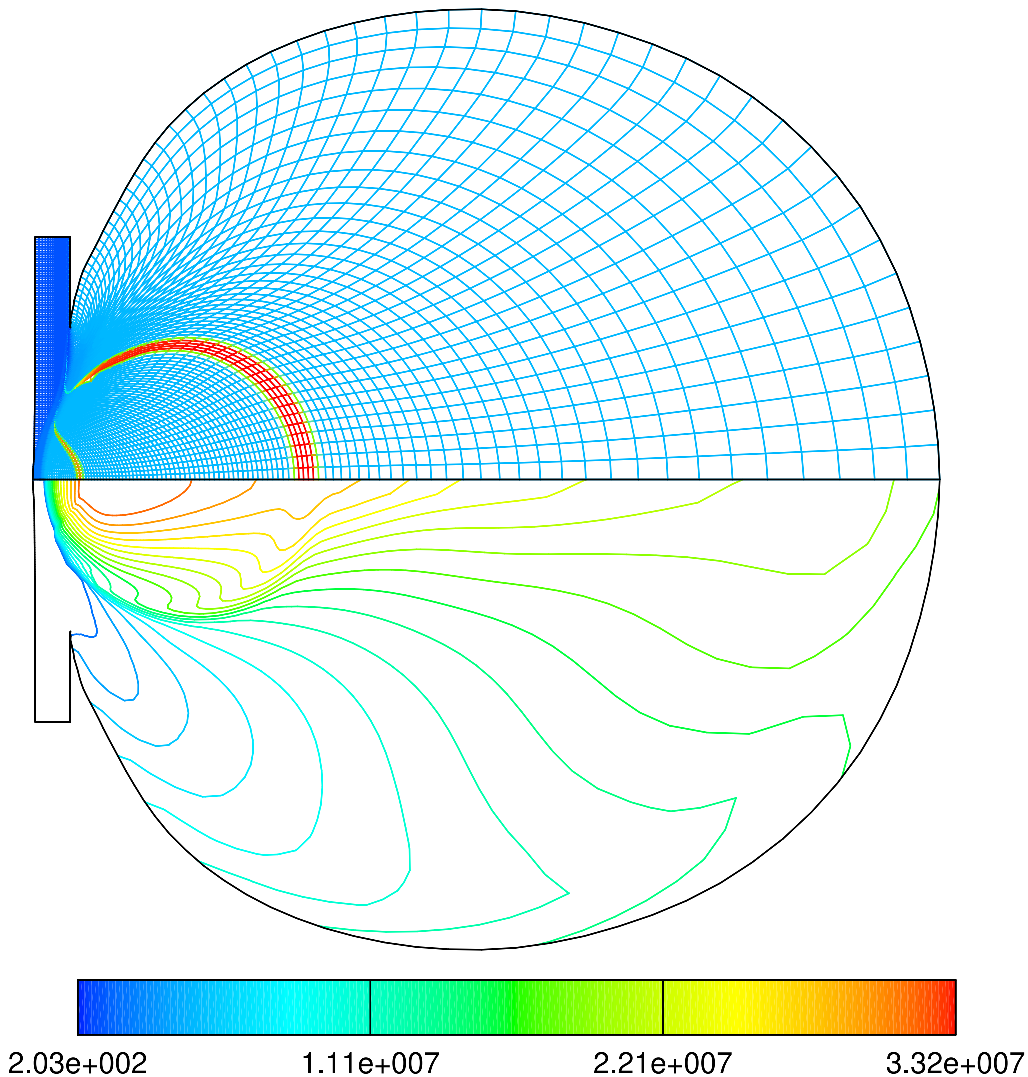

Conclusions and perspectives

- An accurate and robust 2D cell-centered unstructured second order ALE scheme
- Coupling with diffusion scheme (ICF code)
- Concentration equations with mixture assumptions
- Future works
  - Improvement of the mesh relaxation strategy
  - Coupling with interface reconstruction (cf. S. Galera's talk)